THE JOURNAL OF PHYSICAL CHEMISTRY B

ARTICLE

pubs.acs.org/JPCB

Is There Elliptic Distortion in the Light Harvesting Complex 2 of Purple Bacteria?

Seogjoo Jang*

Department of Chemistry and Biochemistry, Queens College of the City University of New York, 65-30 Kissena Boulevard, Flushing, New York 11367-1597, United States

Robert J. Silbey

Department of Chemistry, Massachusetts Institute of Technology, Cambridge, Massachusetts 02139, United States

Ralf Kunz, Clemens Hofmann, and Jürgen Köhler

Experimental Physics IV and Bayreuth Institute of Macromolecular Research (BIMF), Universität Bayreuth, 95447 Bayreuth, Germany

ABSTRACT: Single molecule spectroscopy (SMS) revealed an unusually large Gap between two major exciton peaks of the B850 unit of light harvesting complex 2 (LH2), which could be explained assuming elliptic distortion or $k = 2$ symmetry modulation in the site excitation energy. On the basis of extensive simulation of the SMS data and ensemble line shape, we found that uniform modulation of $k = 2$ symmetry cannot explain the dependence of intensity ratios on the Gap of the two major peaks, which are available from SMS, nor the ensemble line shape. Alternative models of disorder with $k = 1$ and $k = 2$ symmetry correlation are shown to reproduce these data reasonably well and can even explain the Gap distribution when it is assumed that the lower major peak in the SMS line shape is an intensity weighted average of $k = 1-$ and $k = 0$ states.

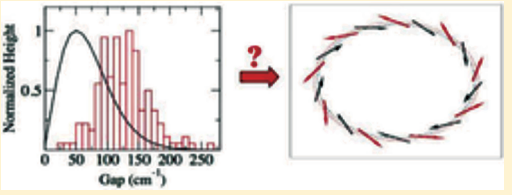

I. INTRODUCTION

How plants harvest photons from sunlight is a question that continues motivating various spectroscopic and theoretical studies. One of the most highly studied systems in this quest is the light harvesting complex 2 (LH2) of purple bacteria for which the determination of X-ray structure in 1995[1,2] has generated a surge of experimental and theoretical investigations.[3,4] These studies provided convincing evidence for the substantial delocalization of the exciton of the B850 unit in LH2. However, direct experimental confirmation of such a delocalized exciton state had remained difficult to obtain. The single molecule spectroscopy (SMS)[5−7] of LH2 by van Oijen et al. was a significant breakthrough in this sense because it clearly demonstrated distinctive excitonic peaks characteristic of the delocalized exciton states for the B850 unit.

While most of the SMS data[5] could be understood by the Frenkel exciton model based on the X-ray crystal structure and simple Gaussian site energy disorder, one feature, the large Gap between two major peaks in each SMS line shape of the B850 unit, was not easy to explain. For this, a new structural model of LH2 with elliptic distortion was proposed.[5] Since then, follow-up justifications[8] and relevant theoretical analyses[9,10] were made. Most recently, an improved model that assumes elliptic modulation in the site energy[11] rather than in the structure was developed. While this latest model seems to provide a satisfactory description of most SMS data, its test against other ensemble/subensemble spectroscopic data has not yet been made.[3,12,13]

Because of the fragile nature of Frenkel exciton and the complexity of the biological system, it is possible that fine details of structural and disorder models may vary with each spectroscopy and sample. However, because of the fact that the disorder in LH2 is of intermediate magnitude at most, such differences in general do not cause significant qualitative changes in many spectroscopic data. In this sense, the large Gap distribution observed from SMS is distinct, and more comprehensive theoretical examination of its implication is needed. In this examination, the following two questions arise naturally: (1) Is the sample of LH2 used for SMS different from those used in typical ensemble spectroscopy? (2) If ensemble spectroscopy is conducted for the same sample of SMS, can it be also explained by the same model of elliptic distortion? We intend to provide more definite answers for these questions as well.

On the basis of the exciton Hamiltonian and exciton-bath Hamiltonian developed previously, we here conduct comprehensive modeling of SMS data and ensemble line shapes. For the latter, the second order time-nonlocal Quantum Master Equation (QME) is used. Four representative models of disorder are

Received: March 11, 2011
Revised: August 9, 2011
Published: September 30, 2011

tested in detail. Both SMS data and the ensemble line shape taken for the sample are used in order to check the consistency of the model. The implications of the present study are provided in the Conclusions.

II. IMPLICATIONS OF THE RESULTS OF THE SMS DATA

According to the X-ray crystallography,[1,2] LH2 is a cylindrically shaped protein−chromophore complex consisting of two groups of circularly arranged bacteriochlorophylls (BChls) with 8- or 9-fold symmetry. These two circular modules absorb photons at about 800 and 850 nm at room temperature and are thus named B800 and B850. A great deal of structural and spectroscopic information on these units is available now.[3,4,6] The LH2 of *Rhodopseudomonas acidophila* studied by van Oijen et al.[5] has 9-fold symmetry, where the B850 unit consists of 9 pairs of BChls attached to α and β polypeptides. In the absence of disorder, the Hamiltonian representing single exciton states of B850 is given by

$$H_e^0 = \sum_{n,m=1}^{9} \sum_{s,s'=\alpha}^{\beta} J_{ss'}(n-m)|s_n\rangle\langle s'_m| \quad (1)$$

where $J_{\alpha\alpha}(0) = \varepsilon_\alpha$, and $J_{\beta\beta}(0) = \varepsilon_\beta$, the excitation energies of α and β BChls. Otherwise $J_{ss'}(n-m)$ represents the resonance coupling between site excitation states $|s_n\rangle$ and $|s'_m\rangle$.

In reality, there are disorder and defects in the protein−chromophore complex, which result in an additional disorder term, δH_e. Thus, the total electronic Hamiltonian becomes

$$H_e = H_e^0 + \delta H_e \quad (2)$$

Though significant, the matrix elements of δH_e are comparable in magnitude to the off-diagonal elements of H_e^0. In this case,[14] the eigenstates of H_e retain the major double band structure of H_e^0 and can be classified as $|\psi_{l,p}\rangle$ and $|\psi_{u,p}\rangle$ with $p = 0, ..., 8$, where l (u) represents the lower (upper) band, as follows:

$$H_e = \sum_{p=0}^{8} \{\varepsilon_{l,p}|\psi_{l,p}\rangle\langle\psi_{l,p}| + \varepsilon_{u,p}|\psi_{u,p}\rangle\langle\psi_{u,p}|\} \quad (3)$$

In the above equation, the convention is that $\varepsilon_{l,p} < \varepsilon_{l,p'}$ and $\varepsilon_{u,p} > \varepsilon_{u,p'}$ for $p < p'$. In the limit where $\delta H_e \to 0$, each of these eigenstates reduces to that of H_e^0 with the corresponding exciton wavenumber $k = \pm(p+1)/2$, where integer division is assumed. For example, $|\psi_{l,0}\rangle$ reduces to the $k = 0$ state of the l band of H_e^0, while $|\psi_{l,1}\rangle$ and $|\psi_{l,2}\rangle$ reduce to linear combinations of the $k = \pm 1$ states. As will be described in more detail below, the analysis is focused on these three lowest exciton states, which will be hereafter abbreviated as $|0\rangle$, $|1-\rangle$, and $|1+\rangle$.

The SM line shape (SML)[5] of the individual B850 unit consists of 2−4 distinctive peaks. Out of these, two major peaks appear consistently, which are indicative of the two exciton states, $|1-\rangle$ and $|1+\rangle$, according to their excitation energies and relative polarizations. Thus, defining the Gap for each SML as the difference between the energies of the two peak maxima, it is reasonable to assume that[5,8,11]

$$\text{Gap} = \varepsilon_{1+} - \varepsilon_{1-} \quad (4)$$

Significant number of SMLs contain 1−2 additional peaks[5,8,11] in the higher energy side of the two major peaks, which correspond to higher exciton states. Because these higher excitonic states are not always observable with good resolution and their assignment ($k = \pm 2$ or $k = \pm 3$) is not always obvious, reliable statistical analysis of these states remains difficult.

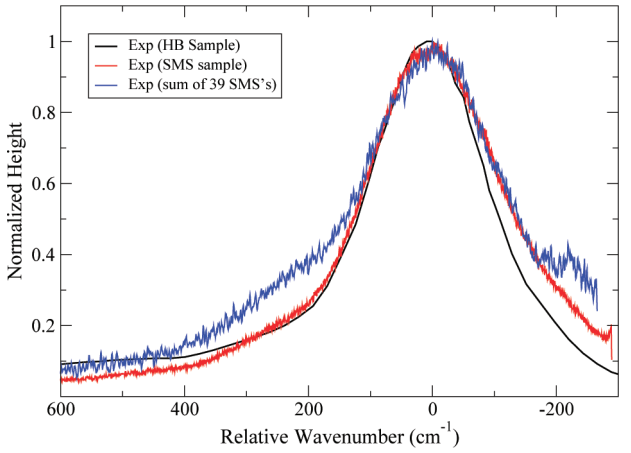

Figure 1. Comparison of the ensemble absorption line shape of B850 obtained from a hole burning sample of LH2 (the Small group[13]) at 4 K, and the fluorescence−excitation ensemble line shape (or sum of 39 SML's) for a sample of LH2 used in the SMS at 1.4 K.

With the assignment of eq 4, van Oijen et al.[5] were able to collect the information on the distribution of the splittings between ε_{1+} and ε_{1-}. It turned out that the resulting experimental distribution had a much larger average and variance than those predicted from the exciton model based on the X-ray structure.[1] In order to explain this discrepancy, van Oijen et al.[5,8] suggested elliptic deformation of the LH2 ring. Later, Hofmann et al.[11] analyzed a more extensive set of single molecule spectroscopy (SMS) data and came up with an improved model that assumes the elliptic modulation (more precisely, modulation of the $k = 2$ symmetry) in the excitation energies of chromophores, which were shown to explain more extensive features of the SMS data.

Even if the modulation is not physical but rather in the site excitation energy, the assumption of the $k = 2$ symmetry modulation is somewhat unusual nor has it been supported by other types of spectroscopy. Does this indicate an unusual sensitivity of the SMS, or is it possible that the sample used in the SMS is qualitatively different from those used in other spectroscopy? Comparison of the ensemble line shapes of B850 for different samples is important in answering this question.

Figure 1 compares two ensemble line shapes of the B850 unit. One is the fluorescence−excitation ensemble line shape taken for the sample[11] used for the SMS at 1.4 K. The other is the conventional absorption line shape taken by the Small group[13] at 4 K for a sample used for hole burning (HB) spectroscopy. Extra care was taken to minimize the disorder in this sample. Though not dramatic, a clear difference can be seen between the two ensemble line shapes, especially on the lower energy side of the peak. This difference is too big to be attributed to the small temperature differences and clearly indicates that the two samples have different types or magnitudes of disorder. Figure 1 also shows the explicit sum of 39 SMLs[11] used for the statistical analysis, which shows some discrepancies from both ensemble line shapes. This indicates that the subset of B850 units employed for the statistical analysis of SMS might be biased toward certain types of disorder.

Table 1. Four Models of Disorder in the B850 Exciton Hamiltonian[a]

	$\varepsilon_\alpha - \varepsilon_\beta$	σ_c	$\sigma_{\alpha(\beta)}$	$E_{mod}^{k=2}$	$\sigma_E^{k=1}$	$\sigma_E^{k=2}$
A	240	50	117	163	0	0
B	0	30	190	0	0	0
C	0	20	210	0	90	90
D	0	30	210	0	180	0

[a] ε_α and ε_β represent the average site excitation energies of α and β BChls. The symbol σ represents the standard deviation of each Gaussian disorder; thus, σ_c is for the ground state energy (or intercomplex disorder), $\sigma_{\alpha(\beta)}$ is for the $\alpha(\beta)$ site excitation energy, and $\sigma_E^{k=1}$ and $\sigma_E^{k=2}$ are those for the amplitudes of correlated site energy disorders with $k = 1$ and $k = 2$, respectively. $E_{mod}^{k=2}$ is the magnitude of the $k = 2$ symmetry modulation of the site energies. All the numbers are in the units of cm^{-1}.

III. MODEL OF ELLIPTIC MODULATION

The exciton Hamiltonian employed by Hofmann et al.[11] is a simplified one that treats α and β BChls equivalently, except for the site energy. Here, we construct the elliptic distortion model based on a more realistic exciton Hamiltonian, eqs 1 and 2. In the notation of the present work, the model of the $k = 2$ site energy modulation suggested by Hofmann et al.[11] can be represented by the following disorder Hamiltonian:

$$\delta H_e = \sum_{n=1}^{9} \{(\xi_{\alpha_n} + E_{mod}\cos(2\cdot 2n\pi/9) - \xi_c)|\alpha_n\rangle\langle\alpha_n| + (\xi_{\beta_n} + E_{mod}\cos(2\cdot(2n+1)\pi/9) - \xi_c)|\beta_n\rangle\langle\beta_n|\} \quad (5)$$

where ξ_{α_n} and ξ_{β_n} represent Gaussian random variables in the site excitation energies of α_n and β_n BChls, and ξ_c is that of the ground electronic state in each complex (so-called intercomplex disorder). E_{mod} is the magnitude of the modulation of the $k = 2$ symmetry in the site excitation energy. A range of parameters were tested for this type of disorder and modulation. We found that the set of parameters[25] shown in list A of Table 1 produce results similar to those obtained by Hofmann et al.[11] Figure 2 shows simulation results, which were obtained by sampling over 1,000,000 realizations of disorder.[26] The experimental results of SMS are also shown for comparison.

In Figure 2, the agreement between experiment and simulation is reasonable for three distributions: the distribution of the Gap defined by eq 4, that of the intensity ratios between the two major peaks, and that of their relative polarization angles. While these confirm the findings of Hofmann et al.,[11] they do not guarantee that model A can also explain other information extracted from the SMS data. As an example, we considered the correlation between the intensity ratio and the Gap. The experimental results are shown in the right bottom panel of Figure 2. Red dots represent all the experimental data points obtained from SMS, and the red dashed line represents the lowest order statistical data, the average intensity ratio vs the Gap. Although the statistics are not satisfactory, the experimental trend is that the intensity ratio decreases as the Gap increases. Compared to this is the theoretical value of $\langle I_{1+}/I_{1-}\rangle$ vs Gap calculated from the simulation, which is shown as a blue dashed line. It is clear that the theoretical value is significantly larger than the experimental one and is insensitive to the value of Gap.

In most SMLs, the peak for the $|0\rangle$ state is not easy to identify. One of the reasons for this may be that the $|0\rangle$ peak is merged

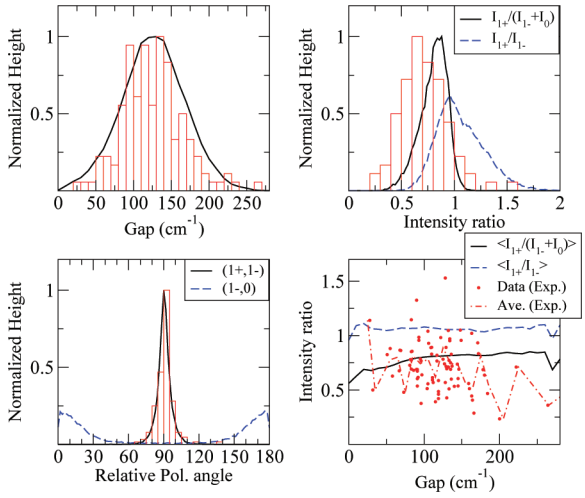

Figure 2. Simulation results and experimental SMS data for model A in Table 1. The top left panel shows the distribution of the Gap, the top right panel shows the distribution of the intensity ratios, the bottom left shows the distribution of the relative polarization angles, and the bottom right shows the correlation between the intensity ratio and the Gap.

with the $|1-\rangle$ peak. Indeed, the comparison of intensity ratios in the top right panel of Figure 2 shows that the experimental distribution of the ratios of the higher to lower major peaks agrees better with the distribution of the intensity ratios, $I_{1+}/(I_{1-} + I_0)$. Thus, we calculated $\langle I_{1+}/(I_{1-} + I_0)\rangle$ as a function of the Gap from the simulation data, which is shown as a black solid line. This average value is closer to the experimental value. However, the trend with respect to the value of the Gap is opposite. Thus, the experimental trend cannot yet be well explained.

Another important test of model A is to examine whether the theoretical ensemble line shape based on the model agrees with the experimental ensemble line shape *taken for the same sample*. Ketelaars et al.[15] made such a comparison but found significant discrepancy. They attributed this to the effect of exciton−phonon coupling, which was not considered in their theoretical modeling.[15] This motivates the need to calculate a more reliable ensemble line shape including the effect of electron−phonon coupling.

IV. EXCITON BATH MODEL AND ENSEMBLE LINE SHAPE

The effects of coupling between electronic excitations and protein phonon modes in B850 can be accounted for by a total Hamiltonian $H = H_e + H_{eb} + H_b$, where H_b represents the phonon bath and H_{eb} the exciton-bath coupling. It is assumed that the bath Hamiltonian can be modeled by an infinite number of harmonic oscillators with a well-defined spectral density and that H_{eb} is linear in the bath coordinate.[16]

At the level of a second order Quantum Master Equation (QME), the ideal line shape[16] of a single B850 complex (the line shape of a single B850 in the absence of quasistatic disorder) can be calculated by the following expression:

$$I(\omega) \approx -\frac{1}{3\pi}\sum_{\hat{e}=\hat{x},\hat{y},\hat{z}} \mathrm{Im}\, Tr_e\left\{\frac{\hat{e}\cdot|D\rangle\langle D|\cdot\hat{e}}{\omega + (\epsilon_g - H_e)/\hbar + i\hat{\mathcal{K}}(\omega)}\right\} \quad (6)$$

where Im means taking the imaginary part of the complex function, Tr_e represents the trace operation of the electronic

degrees of freedom only, ϵ_g is the electronic ground state energy of each BChl, $\hat{\mathbf{e}}$ is the polarization of the radiation, $|\mathbf{D}\rangle = \sum_{n=1}^{9}\sum_{s=\alpha}^{\beta} \boldsymbol{\mu}_{s_n}|s_n\rangle$ is the superposition of the exciton states weighted by the transition dipole vectors, and

$$\hat{\mathscr{K}}(\omega) = \sum_{n=1}^{N}\sum_{p=0}^{8}\sum_{b=l}^{u} \hat{\kappa}(\omega - \epsilon_{b,p}/\hbar) \sum_{s=\alpha}^{\beta} |C_{n,p}^{s,b}|^2 |s_n\rangle\langle s_n| \quad (7)$$

In the above expression, $\hat{\kappa}(\omega)$ is the Fourier transform of the time correlation function of phonons coupled to a single BChl and is expressed as

$$\hat{\kappa}(\omega) \equiv \int_0^\infty dt e^{i\omega t} \int_0^\infty d\omega \mathscr{D}(\omega) \times \left\{ \coth\left(\frac{\hbar\omega}{2k_B T}\right) \cos(\omega t) - i \sin(\omega t) \right\} \quad (8)$$

where $\mathscr{D}(\omega)$ is the spectral density[17] of the phonon modes coupled to the Q_y excitation of each BChl and has been shown to be[18] well modeled by the following function: $\mathscr{D}(\omega) = 0.22\omega e^{-\omega/\omega_{c1}} + 0.78(\omega^2/\omega_{c2})e^{-\omega/\omega_{c2}} + 0.31(\omega^3/\omega_{c3}^2)\, e^{-\omega/\omega_{c3}}$ with $\omega_{c1} = 170\ \text{cm}^{-1}$, $\omega_{c2} = 34\ \text{cm}^{-1}$, and $\omega_{c3} = 69\ \text{cm}^{-1}$. It was assumed that $k_B T = 10\ \text{cm}^{-1}$, which serves as the reasonable cryogenic temperature limit. In eq 6, $C_{n,p}^{s,b}$ is the matrix element of the transformation that relates $\{|\alpha_n\rangle, |\beta_n\rangle\}$ with $\{|\psi_{l,p}\rangle, |\psi_{u,p}\rangle\}$ as follows: $|s_n\rangle = \sum_{p=0}^{N-1}\{C_{n,p}^{s,l}|\psi_{l,p}\rangle + C_{n,p}^{s,u}|\psi_{u,p}\rangle\}$ for $s = \alpha,\beta$.

The calculation of $I(\omega)$ for each ω involves that of $\omega + (\epsilon_g - H_e)/\hbar + i\hat{\kappa}(\omega)$, which has the same dimension as the exciton Hamiltonian H_e, followed by numerical inversion. The whole calculation in the spectral region of B850 for each complex can be conducted in tens of seconds. This enables a theoretical ensemble line shape for any model of disorder to be calculated by averaging eq 6 over many realizations of disorder. Averaging over about 40,000 realizations of the disorder took less than a day in a typical single processor workstation.[27]

In calculating the ensemble line shape, Gaussian disorder in the ground state energy (or intercomplex disorder) with a standard deviation of $\sigma_c = 50\ \text{cm}^{-1}$ was assumed, which is somewhat large but is a minimum value necessary to make the theoretical ensemble line shape single-peaked (the whole set of parameters including this parameter is represented as model A in Table 1). The result is compared with the experimental line shape in Figure 3. A significant difference can be seen between the theoretical and experimental ensemble line shapes. The theoretical line shape is broader and decreases much more steeply on the red side than the experimental one. Recent theoretical studies[19,20] suggest inaccuracy of the second order time nonlocal QME approach at room temperature. However, this effect is expected to be small in the cryogenic temperature limit considered here. In addition, the multiphonon effect, which serves as the major source of the theoretical error, is not likely to explain both the discrepancy in the red side of the peak and the width of the line shape being broader than the experimental one.

The discrepancy between the theoretical and experimental ensemble line shapes in Figure 3 is quite substantial when compared with the performance of other alternative models. For example, the ensemble line shape taken for the HB sample by the Small group[13] can be modeled quite well by assuming simple Gaussian disorder only. The parameters of model B in Table 1 is one such example providing good fit of the experimental ensemble line shape. Figure 4 compares the theoretical ensemble line shape calculated by averaging eq 6 over 40,000 realizations

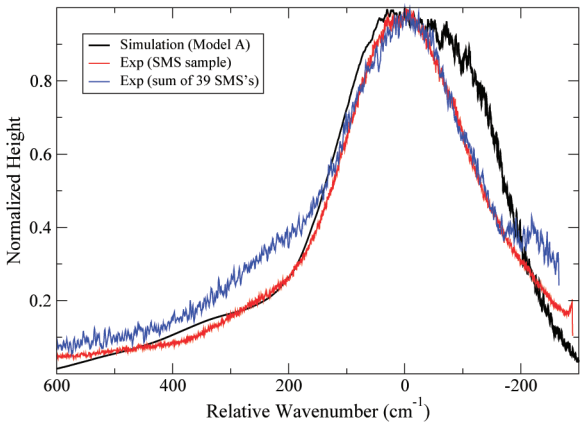

Figure 3. Comparison of the theoretical ensemble line shape (for model A) with the experimental ensemble line shape and the sum of the SMLs.

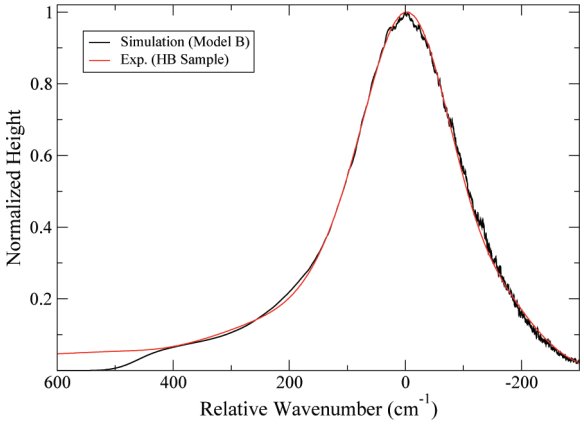

Figure 4. Comparison of the theoretical ensemble line shape (for model B) with the experimental ensemble line shape for a sample used by the Small group in HB spectroscopy. The fall of the theoretical line shape at a value a little above 400 cm^{-1} reflects the fact that the ideal line shape of each B850 unit before averaging over disorder was calculated only up to this value.

of model B disorder with the experimental ensemble line shape. The agreement between theoretical and experimental line shapes is excellent except in the far blue side of the peak where possible multiphonon effects and some contribution of B800 may exist.

For model B, SMS data were calculated by sampling the exciton Hamiltonian over 1,000,000 realizations of the disorder, which are compared against experimental data in Figure 5. As was noted before,[5] the theoretical distribution of the Gap has a much smaller average than the experimental one. The correlation between the intensity ratio and the Gap appears to fit the experimental data better than model A, but the agreement is not yet satisfactory. Considering that different models of disorder are needed for the samples of SMS and HB, these are not unexpected. However, this raises the following question naturally. Is there a model of disorder or distortion that reproduces both the *ensemble line shape* and *other statistical data of the SMS* for the same sample of LH2? Our analysis above shows that model A, which assumes uniform elliptic distortion or $k = 2$ symmetry modulation in the site excitation energy, does not serve that role.

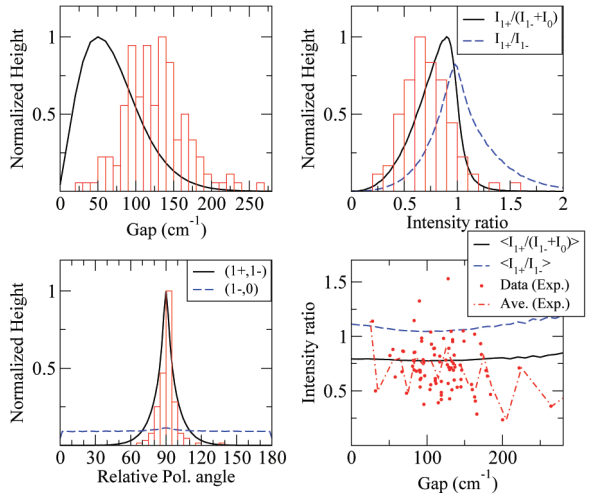

Figure 5. Comparison of the simulation of the SMS data for model B with those of the experimental results. Other details are the same as those in Figure 2.

Thus, it is necessary to consider other alternative models of disorder or distortion to answer this question.

It is plausible to assume that the disorder with the long-range spatial correlation is more dominant than that with the short length scale for the SMS sample of LH2s dispersed on a disordered polymeric surface at the cryogenic temperature limit because the potential barrier associated with the former is expected to be larger than that of the latter. However, there is no specific reason why such long-range disorder have only $k = 2$ symmetry and uniform amplitude. Thus, we here introduce a new model of disorder represented by the following disorder Hamiltonian:

$$\delta H_e = \sum_{n=1}^{9} \{(\xi_{\alpha_n} + \xi_1 \cos(2n\pi/9 + \varphi_{1\alpha}) + \xi_2 \cos(4n\pi/9 + \varphi_{2\alpha}) - \xi_c)|\alpha_n\rangle\langle\alpha_n| + (\xi_{\beta_n} + \xi_1 \cos(2n\pi/9 + \varphi_{1\beta}) + \xi_2 \cos(4n\pi/9 + \varphi_{2\beta}) - \xi_c)|\beta_n\rangle\langle\beta_n|\} \quad (9)$$

where ξ_{α_n} and ξ_{β_n} are the same random Gaussian disorders of the site excitation energy as introduced before, ξ_1 and ξ_2 are random Gaussian variables representing the amplitudes of the correlated disorder in the site excitation energies with $k = 1$ and $k = 2$ symmetries. The standard deviations of these two types of disorder are, respectively, denoted as $\sigma_E^{k=1}$ and $\sigma_E^{k=2}$. In general, four phase variables, $\varphi_{1\alpha}$, $\varphi_{2\alpha}$, $\varphi_{1\beta}$, and $\varphi_{2\beta}$, can be assumed to be arbitrary, and these are sampled from the uniform random variables.

We have tested different sets of parameters and compared the theoretical ensemble line shape with the experimental ensemble line shape of the SMS sample. It was possible to come up with many similar sets of model parameters that can reproduce the experimental ensemble line shape with reasonable accuracy. Model C in Table 1 is a representative of those models of disorder. Figure 6 compares the theoretical ensemble line shape based on this model with the experimental line shapes. The agreement with the experiment is much better than that for model A shown in Figure 3. We also calculated the SMS data, and

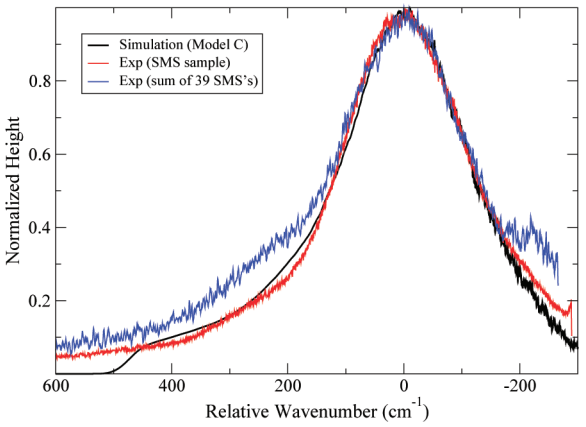

Figure 6. Comparison of the experimental and theoretical ensemble absorption line shapes for model C.

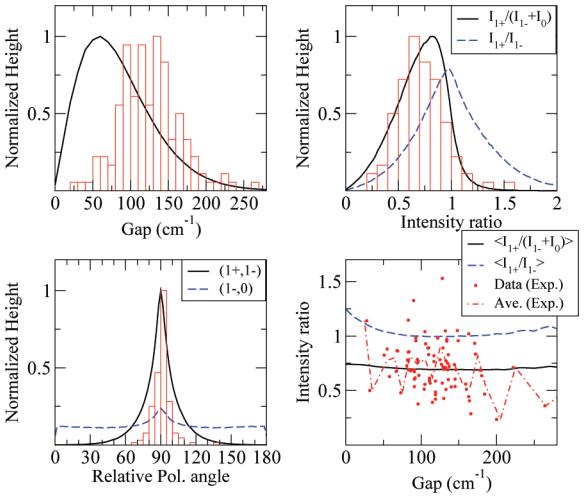

Figure 7. Comparison of the simulation of the SMS data for model C with that of the experimental results. Other details are the same as Figure 2.

the simulation results are compared with experimental data in Figure 7. While other statistical distributions from the SMS are now in reasonable agreement with the experimental data, significant discrepancy can be seen in the distribution of the Gap.

Within the form of the disorder Hamiltonian, eq 9, we also tested another scenario where there is only $k = 1$ symmetry correlation in the site energy disorder and the random Gaussian disorder ($\xi_2 = 0$). On the basis of the test of a range of disorder parameters, we identified a model that reproduces the sum of SMLs (not the ensemble line shape) as closely as possible. This is denoted as model D in Table 1. The resulting ensemble line shape is compared with experimental line shapes in Figure 8. This suggests the possibility that the set of LH2s selected for SMS tend to have larger $k = 1$ symmetry disorder. This is understandable considering that the $k = 1$ symmetry enhances the oscillator strength of the lowest exciton state $|0\rangle$. We also calculated the various statistical distributions that can be obtained from the SMS data. The results are compared with those of the experimental data in Figure 9. As in the case of model C,

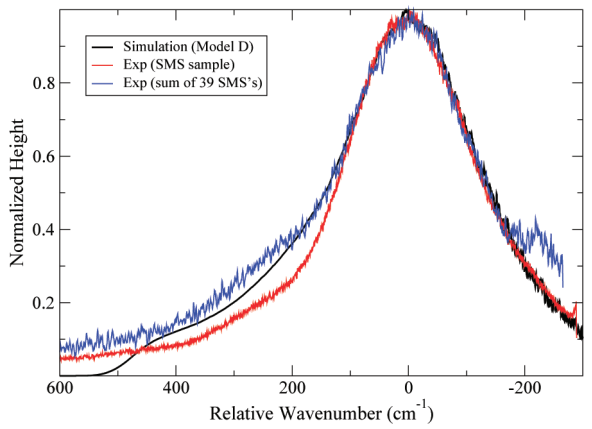

Figure 8. Comparison of the experimental and theoretical ensemble absorption line shapes for model D.

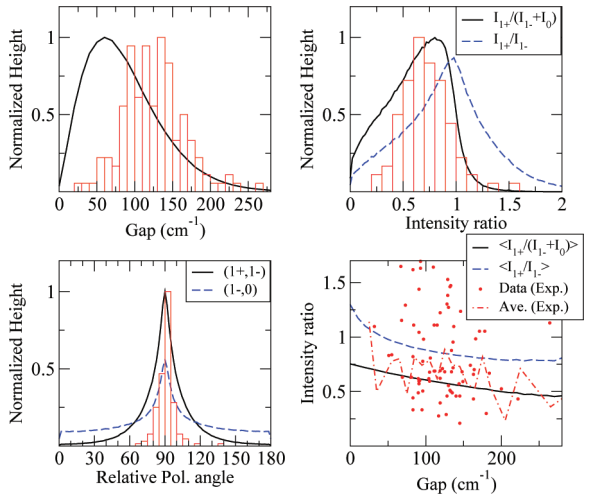

Figure 9. Comparison of the simulation of the SMS data for model D with that of the experimental results. Other details are the same as Figure 2.

the agreement in the Gap distribution is not satisfactory, while others show good agreement with the experimental data.

V. NEW INTERPRETATION OF THE SMS DATA

The results in Figures 7 and 9 show that both models C and D can be viewed as reasonable representations of the SMS data except for the Gap distribution. One may attribute this to the poor statistics of SMS, but it is not likely that only the Gap distribution is subject to such error. Thus, clarification of this issue is necessary. In fact, a careful examination of the analysis made so far suggests an alternative explanation.

In the top right panels of all the figures reporting the simulation of the SMS data for all the models, it is clear that the distribution of the experimental intensity ratios can be modeled better by $I_{1+}/(I_{1-} + I_0)$ than by I_{1+}/I_{1-}. This suggests that the lower major peak in SML contains both contributions from $|1-\rangle$ and $|0\rangle$ states. Therefore, it is not consistent to assume that the $|0\rangle$ state does not affect the peak position of the lower peak at all. If we assume the possibility of dynamical averaging between $|1-\rangle$ and $|0\rangle$ during the time scale of SMS, the position of the lower

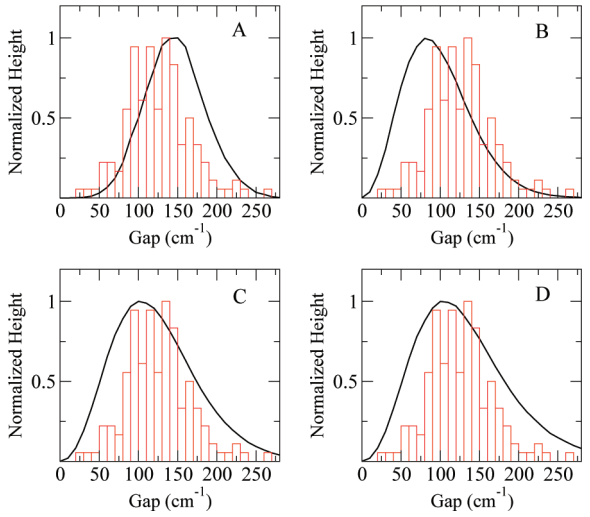

Figure 10. Comparison of the new Gap distributions for four models of disorder in Table 1. Solid lines are simulation results, and the histograms are experimental data.

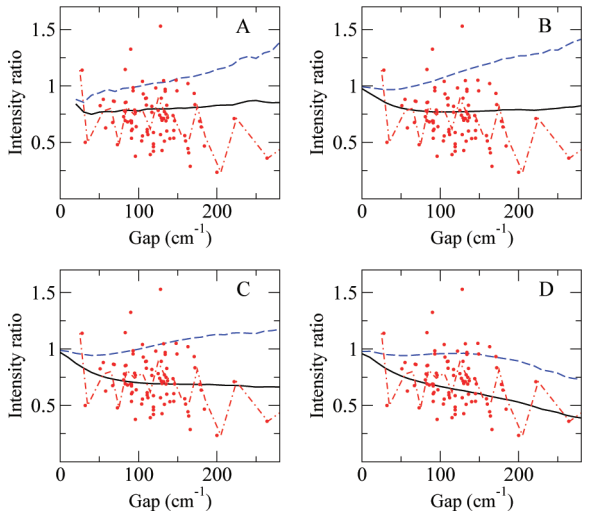

Figure 11. Comparison of the correlation between the intensity ratio and the new Gap for four different models of disorder distribution with two simulation results. The convention is that different lines and dots are the same as the right bottom panel of Figure 2.

peak should be approximated as an intensity weighted average of ε_0 and ε_{1-}. Under this assumption, the Gap measured from the SMS data may indeed be the following quantity:[28]

$$\text{Gap} = \varepsilon_{1+} - \frac{I_0\varepsilon_0 + I_{1-}\varepsilon_{1-}}{I_0 + I_{1-}} \tag{10}$$

Figure 10 shows the resulting Gap distributions for all the four models of disorder and Figure 11 the new intensity-Gap correlations. It is important to note that the new theoretical distributions for models C and D now agree quite well with the experimental data. However, model A now overestimates, and model B still underestimates the Gap distributions. Thus, with the new assignment of the Gap, eq 10, either model C or D can provide a satisfactory description of the full SMS data.

VI. CONCLUSIONS

In this work, we re-examined the interpretation of low temperature SMS data for the B850 unit of LH2. The issue addressed here was whether there is a $k = 2$ symmetry modulation in the site excitation energy of LH2. While this model was capable of explaining most of the SMS data, it has not been clear whether the same assumption can explain other ensemble or subensemble spectroscopic data.

On the basis of a more detailed analysis of the SMS data and theoretical modeling of ensemble line shapes, we came to the conclusion that the assumption of a $k = 2$ symmetry modulation cannot explain the ensemble line shape nor the correlation between intensity ratios of the two major peaks and the Gap. In order to explain these discrepancies, we tested alternative models of disorder, model C, which has disorder with both $k = 1$ and $k = 2$ symmetries, and model D, which has disorder with $k = 1$ symmetry. With the use of the new interpretation of the Gap, eq 10, we found that model C can explain all the SMS data considered and the ensemble line shape taken for the same sample. However, we found that model D can explain all the SMS data and the sum of all the 39 SMS line shapes.

As can be seen from the comparison with model B, which reproduces the ensemble line shape of the Small group, the presence of the additional disorder with $k = 1$ and $k = 2$ symmetry seems to be untrue for any sample. Rather, it is characteristic of the sample used for the SMS, although it does not appear to be caused by a specific method of sample preparation.[21] In addition, the fact that the sum of SMLs can be explained by model D suggests that the selection of complexes tend to be biased toward those with a larger $k = 1$ symmetry disorder and thus with larger fluorescence. However, a comparison of Figures 7 and 8 shows that such bias is not the reason for unusual characteristics of the SMS data.

The types of correlation suggested in the present work are static and long-range and are likely[22] due to the quenched deformation of LH2 from its perfect circular symmetry at low temperature. Thus, they are different from the dynamical and short-range correlation investigated in a recent simulation.[23] Considering the flexibility of proteins constituting the LH2 and the fact that even small distance changes can result in substantial changes in excitation energies of typical molecular systems, the amount of correlated energetic disorder seen for the sample of SMS is in fact very small, which demonstrates the resilience of LH2 in protecting the excitons.

The line shape theory employed here is more suitable for low temperature environments, and different approaches[19,20,24] have been shown to be successful for the modeling of other types of spectroscopy. For example, the hierarchical equation of motion approach[19,20] works well for the modeling of nonlinear spectroscopy at high temperature, and the modified Redfield approach was shown to be successful for modeling single molecule emission spectroscopy.[24] From a theoretical point of view, developing a more satisfactory approach that can encompass a broader temperature regime and dynamical regime is important for the comprehensive understanding of exciton dynamics in LH2.

ACKNOWLEDGMENT

This research was supported by the Office of Basic Energy Sciences, Department of Energy (Grant No. DE-SC0001393). S.J. also acknowledges partial support from the National Science Foundation CAREER award (Grant No. CHE-0846899) and the Camille Dreyfus Teacher Scholar Award. R.K. and J.K. thank the German Science Foundation for financial support (DFG, KO 1359/16 and GRK 1640).

REFERENCES

(1) McDermott, G.; Prince, S. M.; Freer, A. A.; Hawthornthwaite-Lawless, A. M.; Paplz, M. Z.; Cogdell, R. J.; Issacs, N. W. *Nature* **1995**, *374*, 517.
(2) Koepke, J.; X. Hu, X.; Muenke, C.; Schulten, K.; Michel, H. *Structure* **1996**, *4*, 581.
(3) Sundstrom, V.; Pullerits, T.; van Grondelle, R. *J. Phys. Chem. B* **1999**, *103*, 2327.
(4) Hu, X.; Ritz, T.; Damjanovic, A.; Autenrieth, F.; Schulten, K. *Q. Rev. Biophys.* **2002**, *35*, 1.
(5) van Oijen, A. M.; M. Ketelaars, M.; Köhler, J.; Aartsma, T. J.; Schmidt, J. *Science* **1999**, *285*, 400.
(6) Cogdell, R. J.; Gall, A.; Köhler, J. *Q. Rev. Biophys.* **2006**, *39*, 227.
(7) Cogdell, R. J.; Köhler, J. *Biochem. J.* **2009**, *422*, 193.
(8) Matsushita, M.; Ketelaars, M.; van Oijen, A. M.; Köhler, J.; Aartsma, T. J.; Schmidt, J. *Biophys. J.* **2001**, *80*, 1604.
(9) Dempster, S. E.; Jang, S.; Silbey, R. J. *J. Chem. Phys.* **2001**, *114*, 10015.
(10) Mostovoy, M. V.; Knoester, J. *J. Phys. Chem. B* **2000**, *104*, 12355.
(11) Hofmann, C.; Aartsma, T. J.; Köhler, J. *Chem. Phys. Lett.* **2004**, *395*, 373.
(12) Scholes, G. D.; Fleming, G. R. *J. Phys. Chem. B* **2000**, *104*, 1854.
(13) Matsuzaki, S.; Zazubovich, V.; Frase, N. J.; Cogdell, R. J.; Small, G. J. *J. Phys. Chem. B* **2001**, *105*, 7049.
(14) Jang, S.; Dempster, S. E.; Silbey, R. J. *J. Phys. Chem. B* **2001**, *105*, 6655.
(15) Ketelaars, M.; van Oijen, A. M.; Matsushita, M.; Köhler, J.; Schmidt, J.; Aartsma, T. J. *Biophys. J.* **2001**, *80*, 1591.
(16) Jang, S.; Silbey, R. J. *J. Chem. Phys.* **2003**, *118*, 9324.
(17) Renger, T.; Marcus, R. A. *J. Chem. Phys.* **2002**, *116*, 9997.
(18) Jang, S.; Newton, M. D.; Silbey, R. J. *J. Phys. Chem. B* **2007**, *111*, 6807.
(19) Schröder, M.; Kleinekathöfer, U.; Schreiber, M. *J. Chem. Phys.* **2006**, *124*, 084903.
(20) Chen, L.; Zheng, R.; Shi, Q.; Yan, Y. *J. Chem. Phys.* **2009**, *131*, 094502.
(21) Richter, M.; Baier, J.; Cogdell, R.; Köhler, J.; S. Oellerich, S. *Biophys. J.* **2007**, *93*, 183.
(22) Abramavicius, D.; Valkunas, L.; van Grondelle, R. *Phys. Chem. Chem. Phys.* **2004**, *6*, 3097.
(23) Olbrich, C.; Kleinekathöfer, U. *J. Phys. Chem. B* **2010**, *114*, 12427.
(24) Novoderezhkin, V. I.; Rutkauskas, D.; van Grondelle, R. *Biophys. J.* **2006**, *90*, 2890.
(25) In this choice, the assumption of bias, 240 cm^{-1}, in the excitation energy between α and β BChls does not appear to be essential, but we kept this number as close to the model of Hofmann et al. For other models, we kept the bias at zero in order to minimize the set of model parameters.
(26) For reasonable statistics, sampling over about 10,000 is sufficient, but here we conducted averaging over a much larger set in order to minimize ambiguity due to statistical errors.
(27) The resulting theoretical line shape has much more noise on the red side of the peak than the blue side. This is because the major contribution to the red side comes from the peaks of $|1-\rangle$ and $|0\rangle$, which have narrower line widths.
(28) To the best of our knowledge, the possibility that the contribution of the $k = 0$ state may be responsible for the large Gap distribution was raised for the first time by van Grondelle, but systematic investigation of this issue in any publication is not available.